BILINGUAL PUBLISHING CO.
Pioneer of Global Academics Since 1984

Journal of Architectural Environment & Structural Engineering Research
https://ojs.bilpublishing.com/index.php/jaeser

ARTICLE

3D Simulation of Battery Fire on a Large Steel Frame Structure due to Depleted Battery Piles

Nicole Braxtan[1] Jorge Nunez[1] Shen-En Chen[1*] Tiefu Zhao[2] Lynn Harris[3] Dave Cook[4]

1. Department of Civil and Environmental Engineering, University of North Carolina at Charlotte, Charlotte, NC 28223, US
2. Department of Electrical and Computer Engineering, University of North Carolina at Charlotte, Charlotte, NC 28223, US
3. Deutsche Bahn, Raleigh, NC, US
4. Rail Propulsion Systems, Fullerton, CA, US

ARTICLE INFO

Article history
Received: 23 August 2022
Revised: 25 September 2022
Accepted: 11 October 2022
Published Online: 12 October 2022

Keywords:
Lithium ion battery
Train fire
Propagation
Structural safety

ABSTRACT

Lithium ion batteries (LIB) can rupture and result in thermal runaway and battery fires. In the process of transporting lithium ion batteries using trains, the massive collection of batteries can cause train fire and pose significant danger to the public. This is especially critical when the fire occurs amid a heavily populated metropolitan environment. This paper reports the 3D analysis of a warehouse with possible train fire due to LIB rupture and the fire propagation at a rail yard. Six critical fire cases with the battery train in close vicinity to the warehouse were considered. The six fire cases are the worst-case scenarios of a Monte Carlo simulation of different fire cases that may occur to an actual steel storage facility at the Capital Railyard, Raleigh, North Carolina. A 3D finite element (FE) frame model was constructed for the steel warehouse and the most critical fire cases were simulated. The results indicated that several structural components of the warehouse would experience large stresses and deflections during the simulated battery fires and resulting in instability to the structure. Specifically, members of the roof frame represent the most critical elements and that the members can result in large deformations as early as 4 minutes after the fire starts. Furthermore, effective utilization of fire protection can delay somewhat the fire effects and extend time to failure to 45 minutes and in one of the simulated cases, prevent structural instability. Thus, fire from LIB waste transport using train is a very realistic problem due to the thermal runaway, and the analysis performed in current study can be used as a preventive investigation technique for buildings that may be exposed to the train fire risk.

*Corresponding Author:
Shen-En Chen,
Department of Civil and Environmental Engineering, University of North Carolina at Charlotte, Charlotte, NC 28223, US;
Email: schen12@uncc.edu

DOI: https://doi.org/10.30564/jaeser.v5i3.4985

1. Introduction

Li-ion battery (LIB) is currently the energy storage/use technology of choice due to its high energy density and the capability for rapid energy draw [1]. To date, significant amounts of LIBs have been manufactured and used, and the disposal of LIBs is now a critical environmental and safety issue [2]. The disposal of LIBs usually involves transporting them in bulks to either recycling centers where physical separations are performed or straight to landfills [3]. In the US, fire safety of commercial LIBs has been addressed by federal regulations (Federal Register, 2007, 49 CFR parts 171, 172, 173 and 175) [4]. However, no specific guidelines on the transport of spent Li-ion batteries can be found.

Fire impacts due to battery stockpile explosions were raised when in 2017, a double decker rail cargo car carrying lithium ion waste batteries caught fire and exploded in downtown Houston [5]. The incident damaged several residential structures due to the blast shock waves [6]. LIB fires are known to induce damages to nearby structures [7]. The Houston incident instigated the potential danger of fire during mass transport of depleted lithium-ion batteries. In the case of the Houston incident, the fire was propagated to the surrounding area and resulted in nearly an acre of burnt grass field. Figure 1 shows the correlation between battery fire to full-scale locomotive fire as in the case of the Houston train. The inserted curve shows the time history of a single battery cell fire that can rise to maximum temperature in a very short time.

Studies on lithium ion battery fire are limited and design guidelines to prevent fire damage due to lithium ion battery fire are almost non-existent. Thermal runaway, in particular, is one of the failure modes in batteries and distinguishes Lit-ion battery fire from other vehicle fires. For the LIB, thermal runaway is caused by exothermic reactions between the electrolyte, anode, and cathode – with temperature and pressure increasing in the battery, the reaction rate increases due to a temperature increase causing further increases in temperature and hence a further increase in the reaction rate. Eventually, the battery will rupture and may result in an explosion or fire [8,9].

Figure 2 shows the schematic of an operating LIB where electricity is generated when the electrolyte causes chemical changes between the cathode (lithium metal) and the anode (carbon). A thermal runaway (Figure 2b) occurs when the battery experiences a change and several things could happen at the same time: Heating can start, resulting in the breakdown of protective layers and electrolytes, releasing flammable (toxic) gas, resulting in the melting of the separator and leading to short circuit. Finally, the cathode breaks down and generates oxygen and further forces temperature increase. For bulk storage of lithium-ion batteries, the fire propagation can be initiated by battery pack deformation, such as due to a punch-through [10]. Hence, the packaging design of a battery pack plays an important role in preventing cell fire propagation [11].

Thermal runaway is different from conventional fire in that it is fueled by internal exothermic reactions and the supply of oxygen is not essential to the continuation of the chemical process. As a result, the conventional fire extinguishing technique of removing oxygen will not work for LIB thermal runaway. Furthermore, LIB stack fire may result in explosions and the emission of toxic gases, this is evident in the April 19, 2019 battery fire of the AES battery energy storage (BESS) facility in Arizona [12].

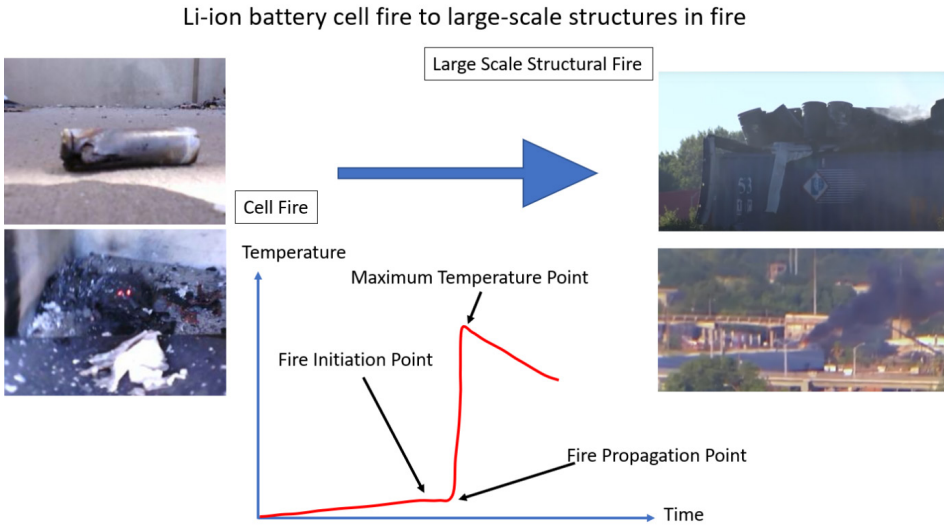

Figure 1. Train Fire due to Battery Cell Thermal Runaway

A review of fire on trains showed that train fire investigation and prevention have been addressed in several publications from the APTA (American Public Transportation Association), including the APTA Recommended Practice for Transit Bus Fire/Thermal Incident Investigation for fire safety analysis of existing passenger rail equipment [13], recommended practices for fire safety [14], for fire protection systems [15], fire safety analysis for existing passenger rail equipment [16] and fire detection technologies [17]. Although these guidelines are not directly related to LIB safety, they can be modified to address fire from Li-ion batteries.

Other fire protection recommendations can be found in publications from the National Fire Protection Association (NFPA) including NFPA 130 [18] which specifically addresses fire protection. For general building structure fire protections, guidelines that may be applicable include the International Building Code [19], which defines fire resistance ratings for buildings based on construction type and building element.

In summary, to ensure fire safety, a fire risk analysis needs to be performed for potential at-risk buildings. The fire risk analysis should result in the identification of the most critical risk scenarios for the safety design of the structure [20]. Detailed structural analysis can then be performed to understand the responses of the structure to the fire risk. To demonstrate a fire risk analysis, this paper describes a fire evaluation performed on an existing steel metal structure with close-by railroads that may be exposed to battery train fires.

In order to assess the responses of the steel frame structure from the worst fire risk case, a nonlinear finite element (FE) fire analysis is conducted based on the most likely fire scenarios from the established fire cases. The worst-case scenarios are established based on a Monte Carlo simulation (fire risk analysis) of more than 5,000 fire cases performed using Cellular Automata. The analysis identified six most critical fire cases. In order to identify the most vulnerable fire propagation event to the structural members, a 3D frame structure model is developed to analyze the steel frame structure which is shown in Figure 3. The most critical fire cases (fire propagating to specific building compartments), derived from the fire risk analysis, were then simulated using the FE model. The 3D analysis allowed a realistic simulation of the fire scenarios and helped indicate the most critical locations for the selected fire scenario. The analysis included steel elements idealized both with and without fire protections to the structure. The analysis process presented in this paper is holistic and consider all likely fire scenarios for the steel frame structure and can be used for any other structures that may be exposed to risks from a LIB fire.

1.1 North Carolina Capital Railyard Warehouse

The steel frame structure is a train repair warehouse at the North Carolina Department of Transportation (NCDOT) Capital Yard in Raleigh, North Carolina. The open-span steel frame structure has metal sidings and roofs and is used for sheltered repair and maintenance works for the Piedmont Railroad serving cities between Raleigh and Charlotte, North Carolina. Two railroad tracks run close (within meters) to the building and a very short track dead-ended partially into the building. The tracks dictated the possible parked positions of a train carrying LIB stockpiles.

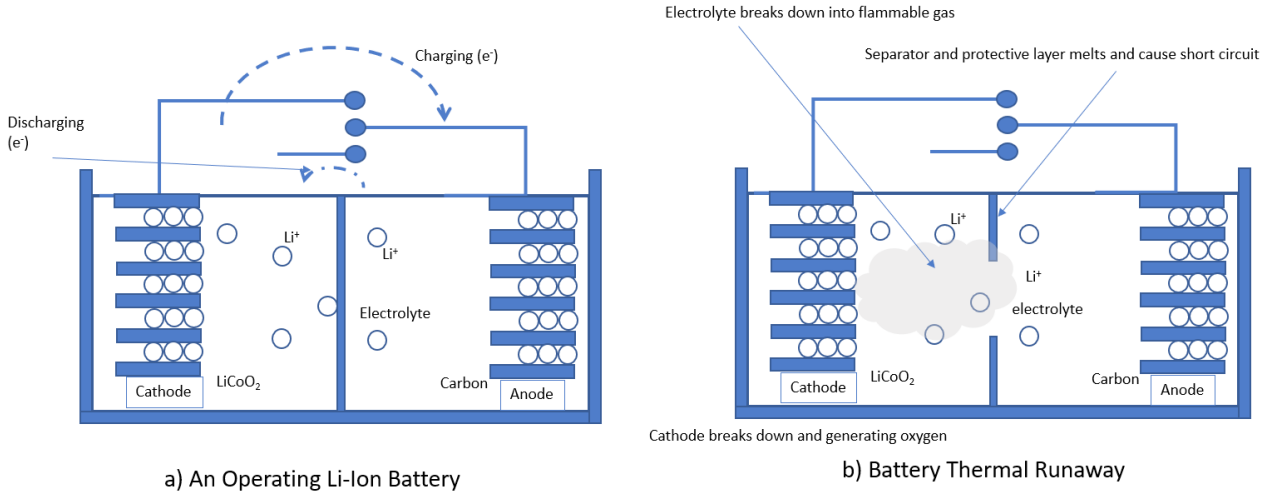

Figure 2. The Li-Ion Battery: a) an Operating LIB cell; and b) LIB Thermal Runaway

a) Exterior of Warehouse

b) Interior of Warehouse

Figure 3. The NCDOT Capital Yard Maintenance Warehouse: a) Exterior and b) interior

The eave height of the warehouse is 7.3 m and the roof is at 9.3 m from the floor slab. Figure 3 shows the steel structure that sits within the NCDOT Capital Yard. The bay width for the floor plan is 7.3 m by 7.9 m. The building is composed of six rigid frames connected with beams and purlins on each roof side between the rigid frames [21-23]. The rigid frame is composed of tapered beams of W18x40's [24]. The purlins are made of C10x25 beams. Figure 4 shows laser scans of the interior of the warehouse. Figure 4a shows the entrance for the train into the building. Figure 4b shows the roofing details of the warehouse. The left side of Figure 4b shows a standalone office structure within the warehouse that was not considered in the numerical modeling. Figure 5 shows the plain view of the original CAD drawing of the building.

Due to the close vicinity of the railroad tracks to the building, hazard arises in that a train filled with disposed LIBs, or a train powered by LIB (hybrid or fully electric), may be parked too close to the structure and potential train fire may propagate to the structure. Hence, a study on the LIB fire risks and the effect of fire on the structure has been performed. The study evaluated the building structure for fire using finite element modeling and a fire risk analysis using an expert opinion approach to establish the risk indices for different fire scenarios, so that the most critical aspects of the building fire can be unpacked for better understanding.

a)

b)

Figure 4. LiDAR Scans of the NCDOT Capital Yard Maintenance Warehouse: a) LiDAR Scan of Warehouse Interior and b) LiDAR Scan of Warehouse Roofing System

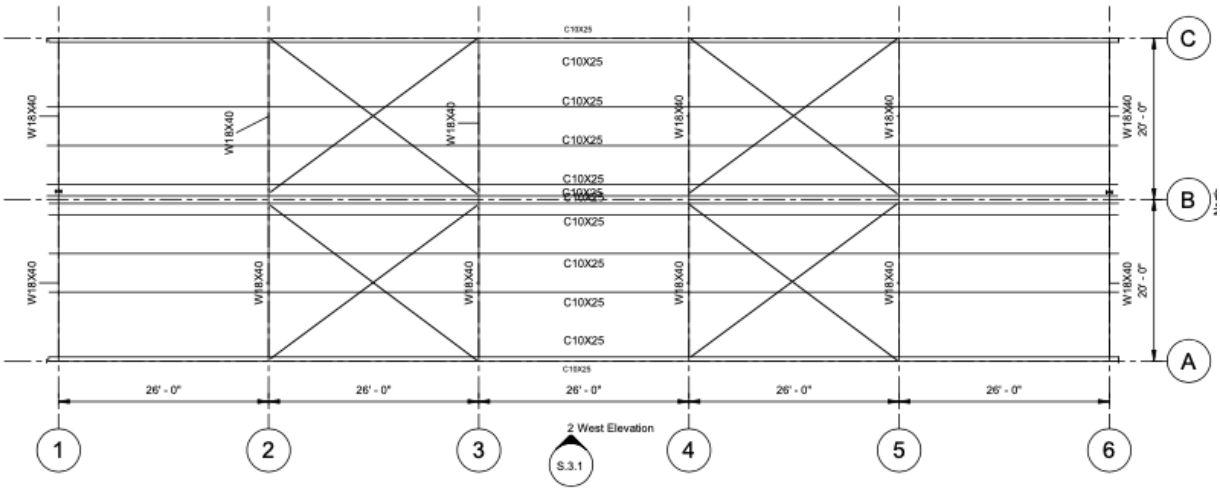

Figure 5. Plan View; Train Warehouse [25]

1.2 Summary of Fire Risk Analysis

The fire risk analysis is conducted using a combination of event probability and severity (risk level), to create a risk rating for a particular event. The probability is scaled from 1 to 5, 1 being frequent and 5 being improbable to occur. The severity aspect is scaled from 1 to 4 where 1 being catastrophic and 4 being negligible. The risk indexing can help prioritize the fire risks, which dictates the structural fire evaluation for the building [25].

The warehouse that is being analyzed in this case study contains fuel, oxygen, and heat source, which are three elements needed in order to ignite a fire. Fire behavior is dependent on the fire temperature, the heat transferred to the surface of the structure, and the corresponding rise of temperature occurring within the structure. Because the warehouse has open space and possible workers within, fire safety will be provided based on the life safety of occupants by identifying the potential fire source and select the best way to control and extinguish the fire at an early stage, and possible extend the time needed for the safe egress of people.

Mira et al. [25] conducted a detailed fire risk analysis wherein the warehouse building was partitioned into 14 exterior and interior compartments, as shown in Figure 6 and described in Table 1. Special considerations for compartments are also included in Table 1 as necessary, dictating additional parameters in the fire ignition and spread potential as well as increased life safety. Current study extends the 2D analysis into 3D and further improve the models to allow the identification of the specific failing members.

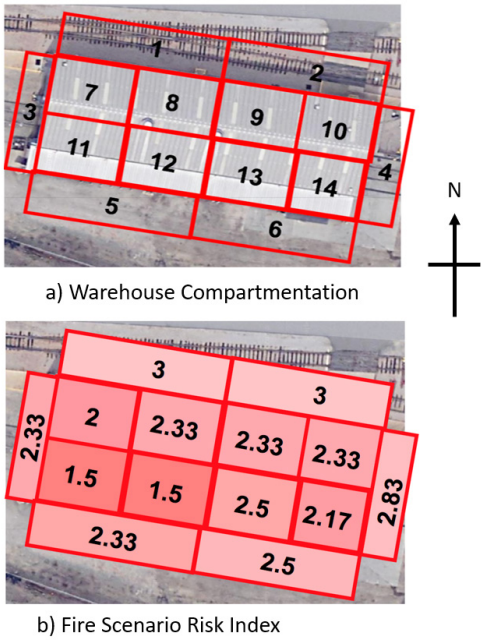

Figure 6. Warehouse Building Compartment Designation [25]

All likely critical elements that may cause fire ignition and spread to the building have been considered, including sources related directly to the LIBs onboard the train and other traditional fire hazards surrounding the building. The fire hazards considered are fire initiated from the train, exterior electric power transformers, power supplies within the warehouse, chemical tanks outside of compartment 13 and 14, overhead transformer fire and a large gas tank behind the building. For this investigation, a total of six specific fire scenarios were considered and used for the fire risk analysis. Each scenario is further identified by

Table 1. Compartment Designations in the Fire Risk Evaluation [25]

Compartment No.	Description	Special Considerations
1	Top left exterior wall (Exterior)	Close proximity exterior tracks
2	Top right exterior wall (Exterior)	Close proximity exterior tracks
3	Middle left exterior wall (Exterior)	Tracks enter into warehouse
4	Middle right exterior wall (Exterior)	Tracks do not enter warehouse
5	Bottom left exterior wall (Exterior)	Adjacent chemical storage
6	Bottom right exterior wall (Exterior)	Wide open door
7	Top left interior structural elements (Interior)	Wide open door
8	Middle top left interior structural elements (Interior)	Power tool storage
9	Middle top right interior structural elements (Interior)	Includes stand-alone office with glass frame (additionally occupancy)
10	Top right interior structural elements (Interior)	Houses electric controls on interior wall
11	Bottom left interior structural elements (Interior)	Railroad tracks extend through for sheltered repair work
12	Middle bottom left interior structural elements (Interior)	Railroad tracks extend through for sheltered repair work
13	Middle bottom right interior structural elements (Interior)	Adjacent chemical storage
14	Bottom right interior structural element (Interior)	Adjacent chemical storage

a numeric number and the detailed description for each scenario is shown in Table 2.

A survey was sent out to individuals seeking expert opinions on the fire cases and the ranking of the cases. The risk index matrix was established where each of the six fire scenarios was individually applied to the compartments of the warehouse. The risk analysis resulted in a total of 84 scenarios. The expert opinion approach involved ten expert members and each ranked the risks independently. The average risks from the collected opinions of the seven members were calculated and then used to rank the different scenarios. The most and least critical areas of the warehouse were then identified. The outcomes are then mapped onto the compartment schematic shown in Figure 6, where the lower risk index values mean higher potential fire risks. From Figure 6b), it is shown that the most significant fire scenario is the fire propagating due to battery train parked inside of the structure and train fire propagating to compartments 11 to 12. The least significant fire scenario is when fire occurring to compartments 7, 8, 9 and 10. Hence, detailed structural fire analysis was conducted to compartments 11 to 13. The compartment 13 was included to extend the fire analysis for multiple bays of the structure.

Table 2. Detailed Fire Scenarios [25]

Fire Scenario	Details
(1) Train Fire Outside*	Ignition: Battery thermal runaway in locomotive. Fire development: Easily igniting material catches on fire. Fire propagation: Fire material smolders and propagate to warehouse.
(2) Train Fire Inside*	Ignition: Battery thermal runaway in locomotive. Fire development: Easily igniting material catches on fire. Fire propagation: Fire material smolders and propagate to warehouse.
(3) Chemical Storage Fire**	Ignition: Storage containment unit ignites. Fire development: Flammable material catches on fire. Fire propagation: Fire material smolders and propagate to warehouse.
(4) Power Electronics Fire**	Ignition: Short circuit of poorly insulated power electronics. Fire development: Flammable material catches on fire. Fire propagation: Fire material smolders and raise temperature.
(5) Transformer Fire**	Ignition: Transformer catches fire due to short circuit. Fire development: Easily igniting material catches on fire. Fire propagation: Fire material smolders and propagate to warehouse.
(6) Gas Containment Fire**	Ignition: Gas containment unit catches on fire. Fire development: Easily igniting material catches on fire. Fire propagation: Fire material smolders and propagate to warehouse.

*Fire starting scenarios associated with train with LIBs

*Fire starting scenarios specific to the NCDOT railyard warehouse

2. Structural Fire Analysis

A 3-D structural finite element model was developed using Abaqus Finite Element Software [26] to investigate high-risk fire scenarios present on the rail warehouse structure. A 3-D frame model was constructed as shown in Figure 7, using two-node cubic beam elements (B33) throughout the model, with tapered cross-sections defined on the column elements and fixed support boundary conditions at the base of the frame [27]. Self-weight was applied using a gravity load in addition to a superimposed dead load of 958 Pa. Both self-weight and superimposed dead load were held constant as the fire load was specified through a temperature field [28] applied to the steel members. General static steps with automatic incrementation and nonlinear geometry were used throughout the analysis.

In lieu of a full heat transfer finite element solution, an iterative, transient heat transfer analysis was performed on the unprotected steel members exposed to fire based on the temperature rise of the steel member, ΔT_s defined in the AISC Specifications [24]:

$$\Delta T_s = \frac{a}{c_s\left(\frac{W}{D}\right)}(T_F - T_s)\Delta t \quad (1)$$

where,

a = heat transfer coefficient, Btu/(ft^2-s-^{o}F)(W/m^2-^{o}C)
$= a_c + a_r$
a_c = convective heat transfer coefficient
a_r = radiative heat transfer coefficient, given as:
$= \frac{S_B \varepsilon_F}{T_F - T_s}\left(T_{FK}^4 - T_{SK}^4\right)$
c_s = specific heat of the steel, Btu/lb-^{o}F (J/kg-^{o}C)
D = heat perimeter, in. (m)
S_B = Stefan-Boltzmann Constant = 5.67 x 10^{-8} SWm^{-2}k^{-4}
T_F = temperature of the fire, ^{o}F (^{o}C)
T_{FK} = temperature of the fire, ^{o}K
= (T_S+459)/1.8 for TF in ^{o}F
= (T_S+273) for TF in ^{o}C
T_S = temperature of the steel, ^{o}F (^{o}C)
T_{SK} = temperature of the steel, ^{o}K
= (T_S+459)/1.8 for TF in ^{o}F
= (T_S+273) for TF in ^{o}C
W = weight (mass) per unit length, lb/ft (kg/m)
ε_F = emissivity of the fire and view coefficient
Δt = time interval, s

The hydrocarbon fire was chosen for the design fire for a large-scale lithium-ion battery fire, offering a fire scenario with more rapid temperature rise and higher temperatures than the standard E119 fire typically used for compartment fires with traditional building material fuel loads. Figure 8b compares the hydrocarbon fire and resulting unprotected steel member temperatures to the temperatures specified in the ASTM E119 Standard fire. Additionally, a modified fire curve was developed to simulate steel members with appropriate fire protection applied where the hydrocarbon fire curve was scaled to limit the temperature of the steel members to 538 °C [25]. The emissivity was assumed to be 0.7, typical of steel structures, and a convection coefficient of 50 W/m^{2}K was used for the hydrocarbon fire [30].

Abaqus *Elastic and *Plastic parameters were used to input temperature-dependent, nonlinear material properties for the steel. Temperature-dependent coefficient of thermal expansion was calculated based on the thermal strain defined in Eurocode [29,30] and is shown in Figure 8b. Density was specified as a constant 7,850 kg/m^3.

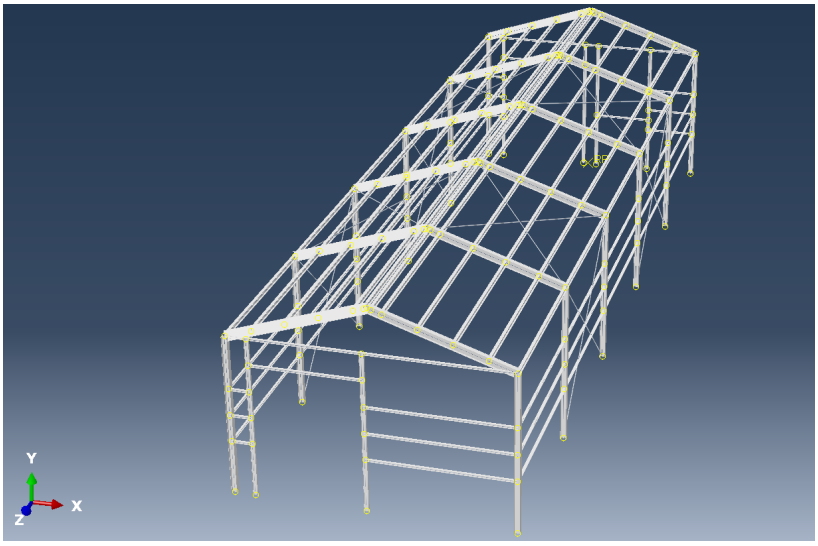

Figure 7. Overall FE Model Geometry

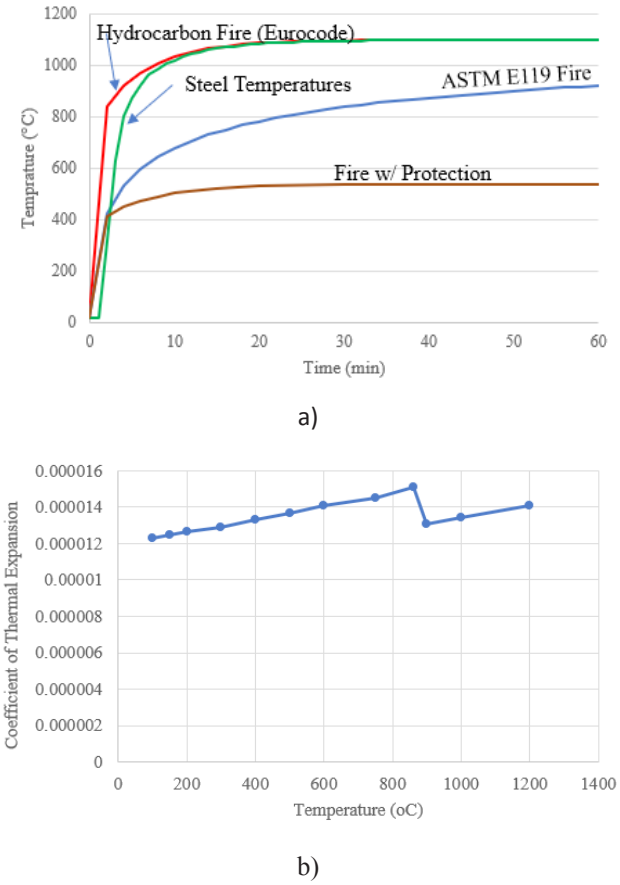

Figure 8. Thermal Characteristics of Fire Used in FE Modeling (a) Fire Curves and Steel Temperatures (b) Temperature Dependent Thermal Expansion [25]

3. Discussion

3.1 Fire Propagation Analysis

Several iterations of FEA models were generated in Abaqus in order to evaluate the warehouse structure under various fire design curves and levels of exposure. The FEA models were based on building dimensions which were generally similar to that of the existing railyard structure, however structural members were modified or replaced to facilitate analysis. The fire design curves used in analysis were limited to the steel temperature fire curve based on heat transfer analysis and the modified fire curve with steel member temperature limited to 538 °C.

The heat transfer analysis curve was assumed to represent steel framing which does not have fire protection and the modified curve was assumed as steel framing with appropriate fire protection. FEA models were identified as "unprotected" and "protected" cases for those consisting of the heat transfer analysis curve and modified fire design curves, respectively, in an effort to create a clear distinction.

As determined by the fire risk analysis, the most significant fire scenarios were related to battery train fire propagating to building compartments. Therefore, FEA models considered the length of a battery train car and the various positions an individual car may occupy within the warehouse. A train car could span anywhere from a single bay in the warehouse up to a total of three bays in length, for which the design fire was first applied to only Bay 11, then Bays 11 and 12, and then Bays 11, 12 and 13. A summary of FEA models is shown in Table 3. As shown in Table 3, the fire protection scenarios are also considered resulting a total of six study cases.

Table 3. FEA Model Summary

Fire Protection	Bays Exposed to Fire	Case
Unprotected (Maximum Design Fire Temperature of 1100 °C)	11	1
	11 and 12	2
	11, 12, and 13	3
Protected (Max Design Fire Temperature of 538 °C)	11	4
	11 and 12	5
	11, 12, and 13	6

The earliest iterations of the Abaqus models were constructed using tapered W18x40 columns along the East and West elevations of the structure, W8x10 columns along the North and South elevations of the structure, W18x40 rafters, C10x25 purlins, and C5x6.7 girts. Analysis of these Abaqus models tended to abort soon after fire was applied to the structural members. The Abaqus software will abort analysis if structural instability is encountered. It was found that these models were improved when wide-flange members were used instead of channels. Therefore, channels were replaced with wide-flange members of a similar section modulus; C10x25 purlins were replaced with W8x21 members and C5x6.7 girts were replaced with W4x13 members.

FE analysis results were obtained from Abaqus in the forms of displacements, Von Mises (Mises) stresses, and temperatures relative to time. Displacements are presented as U1, U2, and U3 which represent deflection in the x, y, and z directions, respectively. Von Mises stresses are presented as SP1, SP5, SP9, and SP13 which is a reference to section points on a cross-section of a wide-flange member as shown in Figure 9. Due to the large amount of data resulting from the analysis, only data from representative nodal points of Purlin and Girt members are included in this paper as these presented the highest levels of stress and deformation. Data for individual nodes for each case are included in Figures 10 through 15. Data for maximum temperature, maximum stress, and maximum absolute deflection for each node is included in Tables 4 through 6,

respectively.

In general, for both the Unprotected and Protected design fire cases it was observed that maximum deflection occurs nearly at the same time as the maximum temperature. Also, maximum stress levels occur within the first four minutes of the design fire for both design fire cases. In most cases, it was observed that members reached stress levels between 241.3 MPa (35ksi) and 337.8 MPa (49ksi), which is near yield-stress for most common grades of steel. Only three nodes, of the fourteen nodes observed, have stress recordings below the yield-stress level yet they had maximum deflections between seventeen and twenty-three inches. These three nodes were part of the unprotected design fire cases.

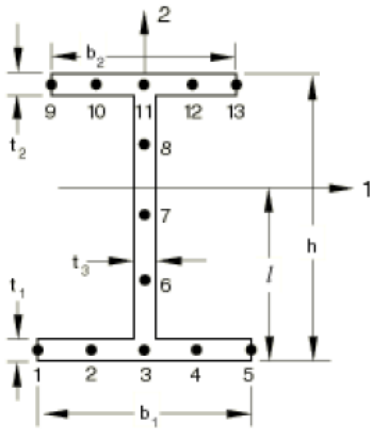

Figure 9. W-Beam Section Points

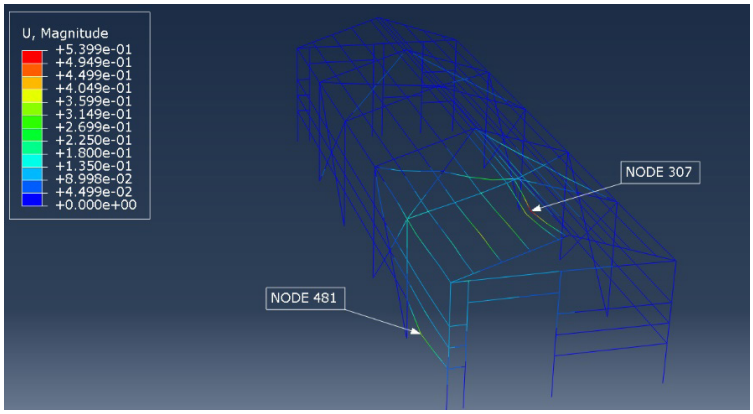

a) Case 1 Node Locations

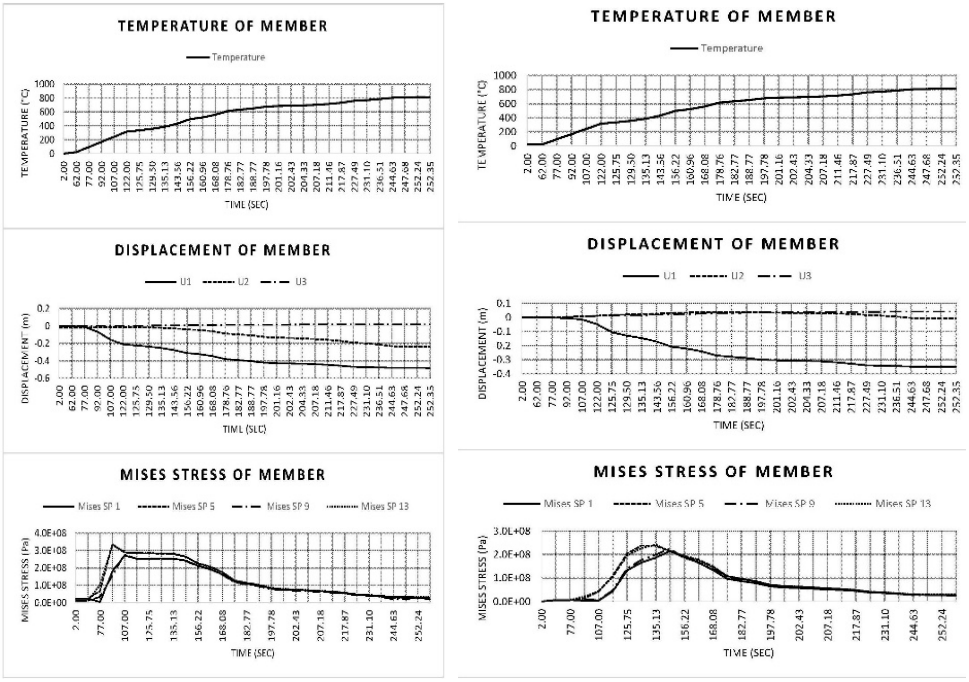

b) Case 1- Purlin Node 307 c) Case 1- Girt Node 481

Figure 10. Case 1 Results

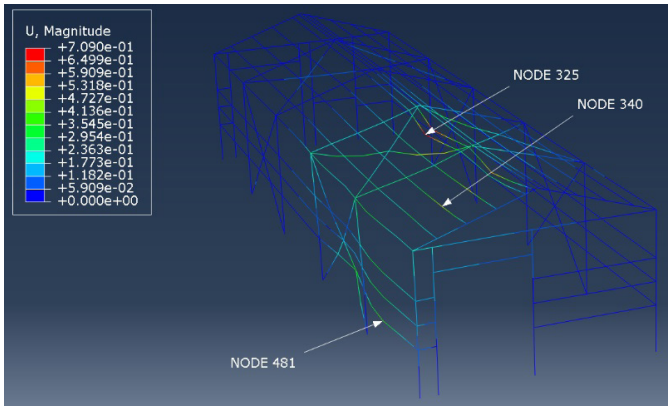

a) Case 2 Node Locations

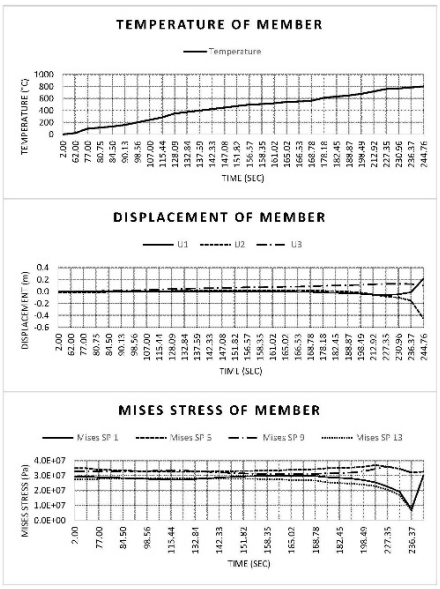

b) Case 2- Purlin Node 325

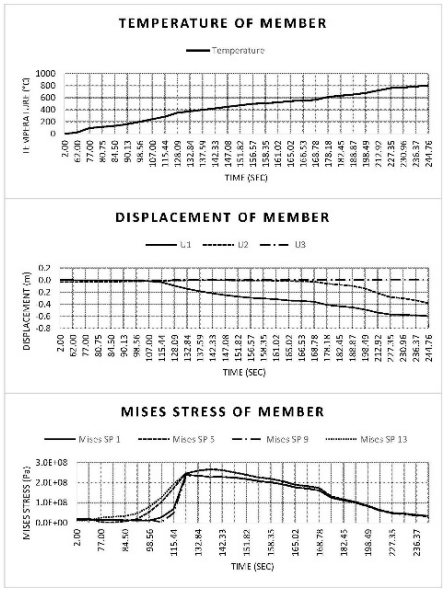

c) Case 2- Purlin Node 340

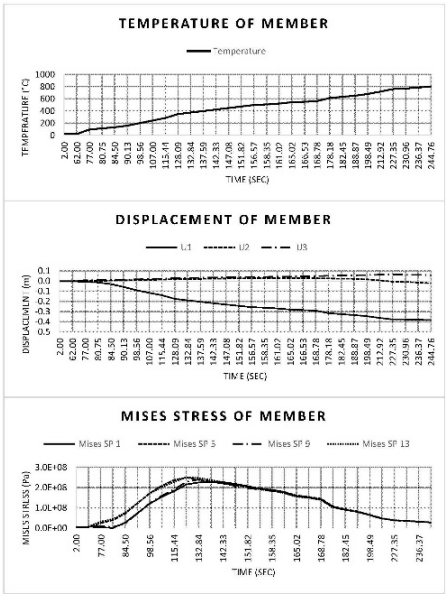

d) Case 2- Girt Node 481

Figure 11. Case 2 Results

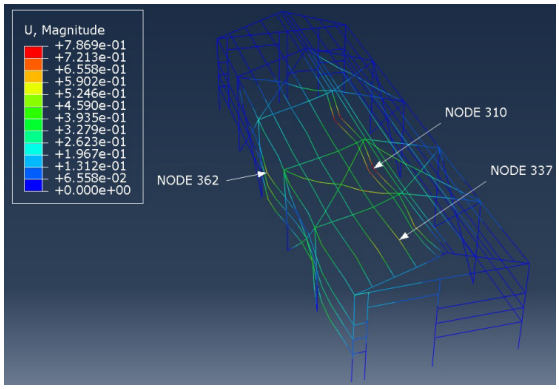

a) Case 3 Node Locations

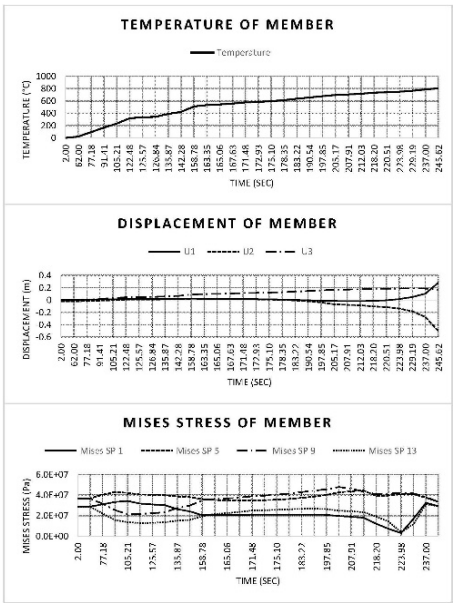

b) Case 3- Purlin Node 310

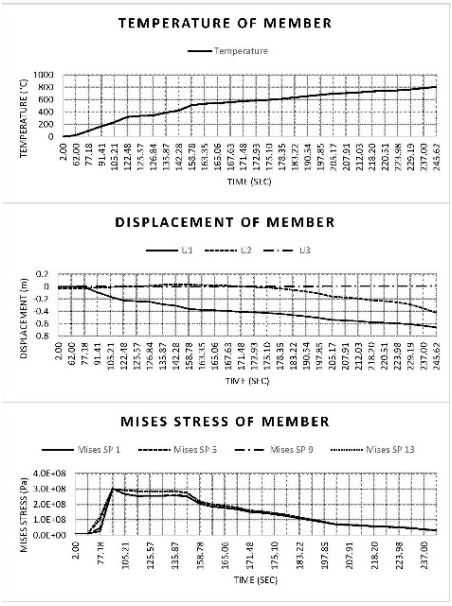

c) Case 3- Purlin Node 337

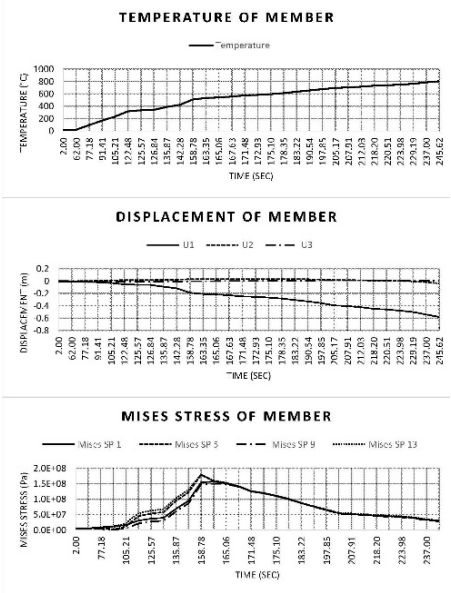

d) Case 3- Girt Node 362

Figure 12. Case 3 Results

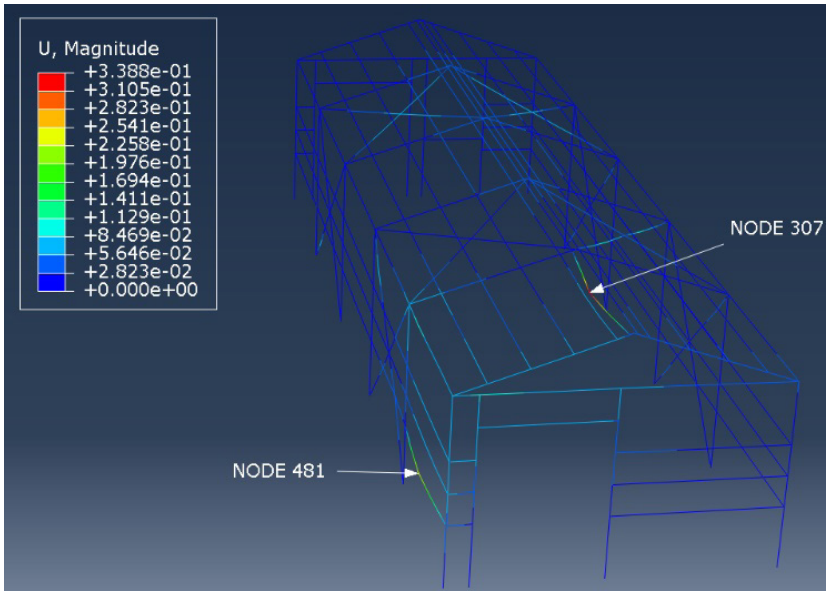

a) Case 4 Node Locations

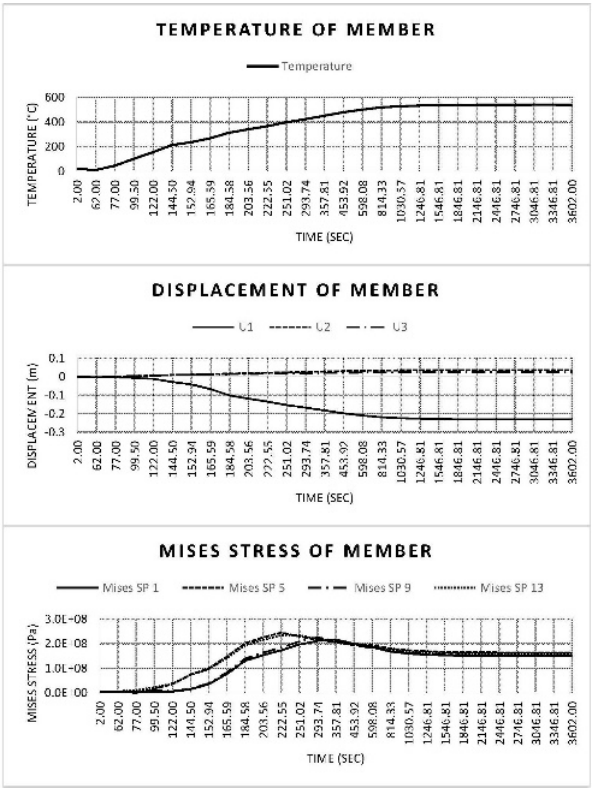

b) Case 4- Purlin Node 307

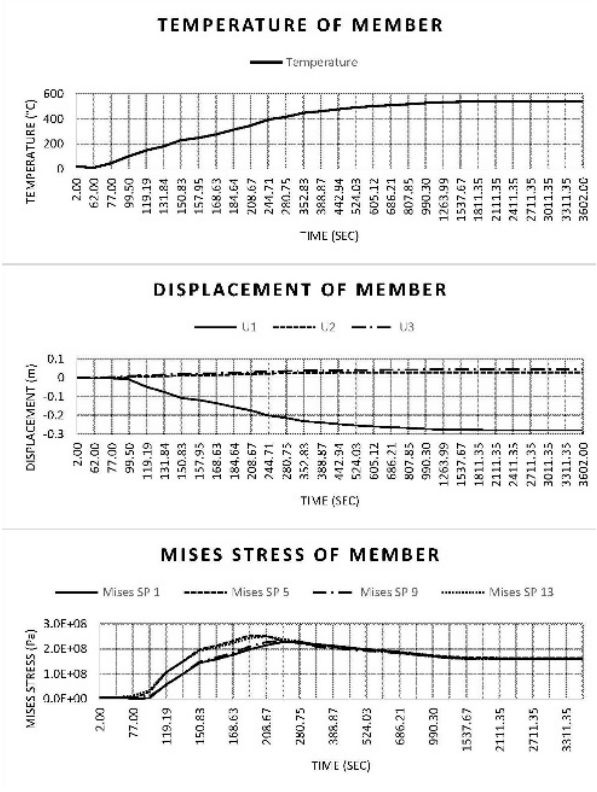

c) Case 4- Girt Node 481

Figure 13. Case 4 Results

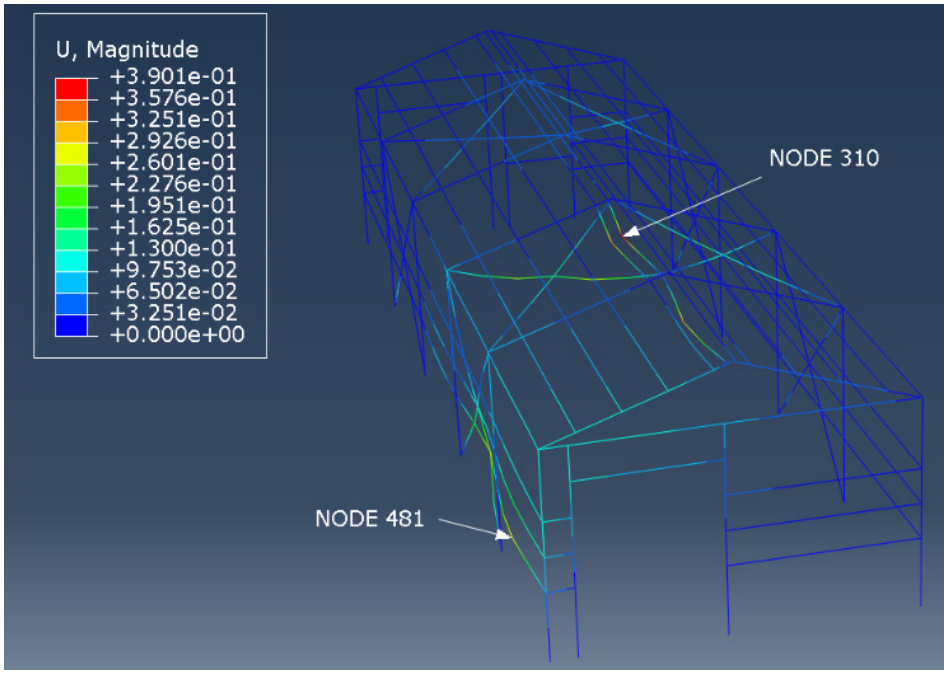

a) Case 5 Node Locations

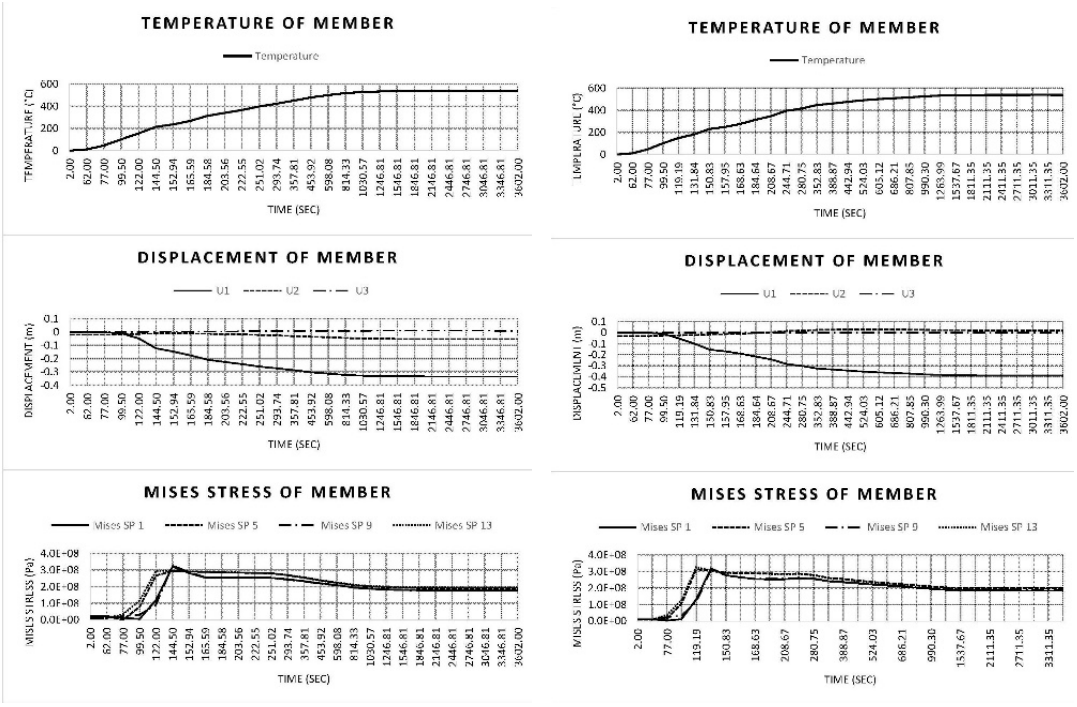

b) Case 5- Purlin Node 310 c) Case 5- Girt Node 481

Figure 14. Case 5 Results

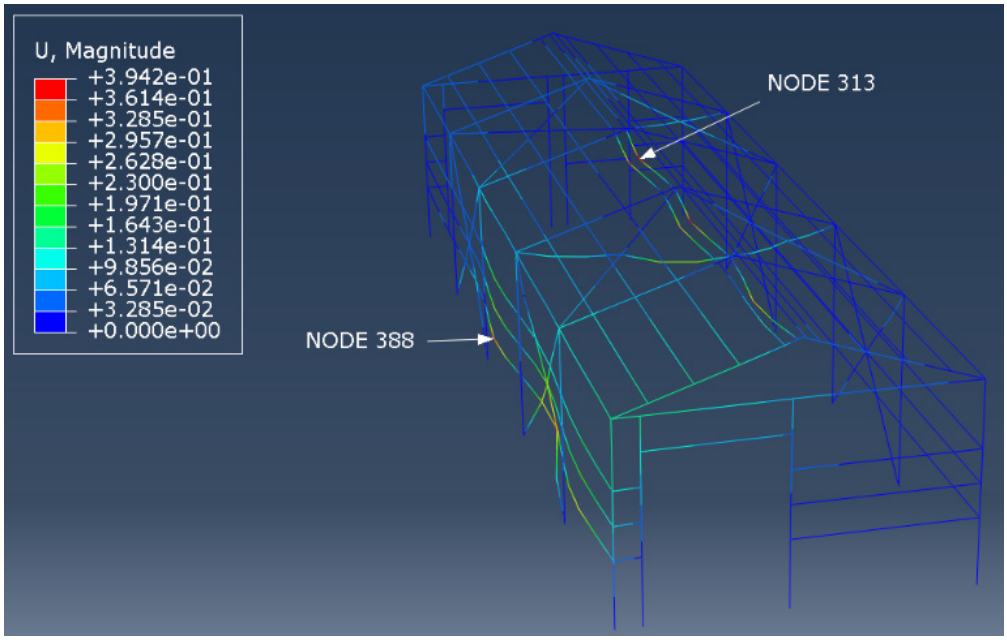

a) Case 6 Node Locations

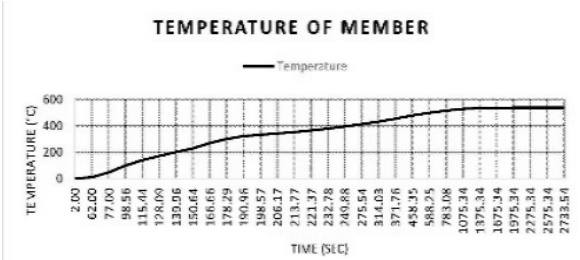

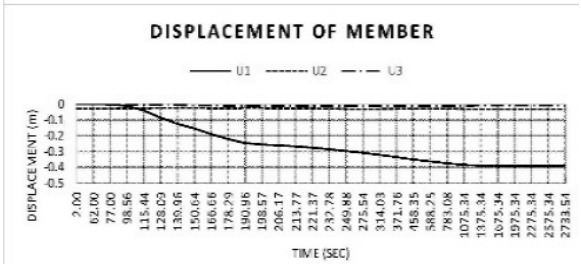

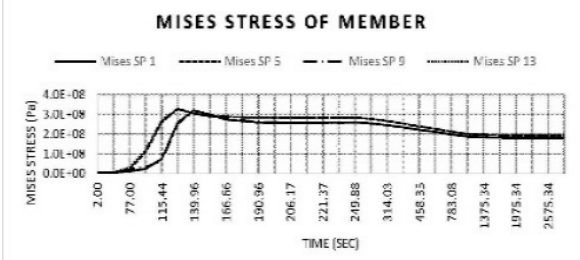

b) Case 6- Purlin Node 313

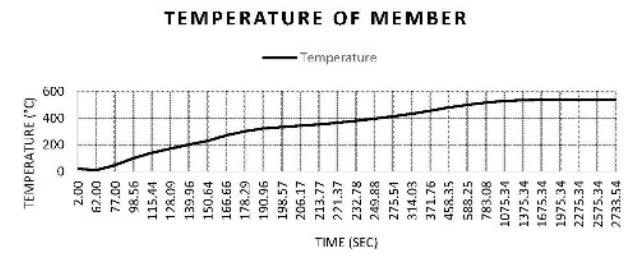

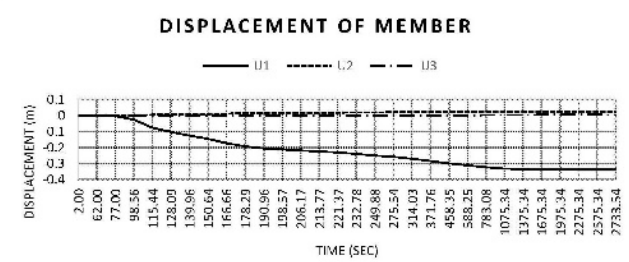

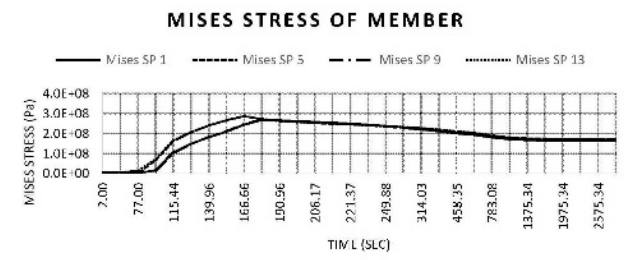

d) Case 6- Girt Node 388

Figure 15. Case 6 Results

Table 4. FEA Model – Maximum Temperature

Fire Protection	Bays Exposed to Fire	Case	Abaqus Model Run Time (sec)	Node Number	Member Type	Maximum Temperature			
						Time (sec)	Displacement (m)	Stress (pa)	Temperature (°C)
Unprotected	11	1	252.4	307	Purlin	252.4	0.4826	3.08E+07	814
				481	Girt	252.4	0.3503	2.90E+07	814
	11 and 12	2	244.8	325	Purlin	244.8	0.5967	3.40E+07	805
				340	Purlin	244.8	0.4552	3.26E+07	805
				481	Girt	244.8	0.3844	2.79E+07	805
	11, 12, and 13	3	245.6	310	Purlin	245.6	0.6614	3.31E+07	806
				337	Purlin	245.6	0.5044	3.34E+07	806
				362	Girt	245.6	0.5808	3.06E+07	806
Protected	11	4	3602	307	Purlin	3602	0.3345	1.95E+08	539
				481	Girt	3602	0.2309	1.64E+08	539
	11 and 12	5	3602	310	Purlin	3602	0.3896	1.99E+08	539
				481	Girt	3602	0.2799	1.64E+08	539
	11, 12, and 13	6	2733.5	313	Purlin	2733.5	0.3927	1.92E+08	539
				388	Girt	2733.5	0.3388	1.73E+08	539

Table 5. FEA Model – Maximum Stress

Fire Protection	Bays Exposed to Fire	Case	Abaqus Model Run Time (sec)	Node Number	Member Type	Maximum Stress			
						Time (sec)	Displacement (m)	Stress (pa)	Temperature (°C)
Unprotected	11	1	252.4	307	Purlin	92	0.0655	3.35E+08	168
				481	Girt	135.1	0.1468	2.42E+08	385
	11 and 12	2	244.8	325	Purlin	137.6	0.1857	2.67E+08	398
				340	Purlin	212.9	0.1216	3.70E+07	719
				481	Girt	128.1	0.1765	2.51E+08	348
	11, 12, and 13	3	245.6	310	Purlin	91.4	0.0925	3.04E+08	165
				337	Purlin	205.2	0.1675	4.78E+07	697
				362	Girt	158.8	0.1875	1.80E+08	510
Protected	11	4	3602	307	Purlin	144.5	0.1229	3.26E+08	213
				481	Girt	222.6	0.1353	2.45E+08	366
	11 and 12	5	3602	310	Purlin	119.2	0.0533	3.27E+08	148
				481	Girt	184.6	0.1569	2.54E+08	313
	11, 12, and 13	6	2733.5	313	Purlin	128.1	0.0865	3.28E+08	171
				388	Girt	166.7	0.1731	2.87E+08	270

Table 6. FEA Model – Maximum Absolute Displacement

Fire Protection	Bays Exposed to Fire	Case	Abaqus Model Run Time (sec)	Node Number	Member Type	Maximum Absolute Displacement			
						Time (sec)	Displacement (m)	Stress (pa)	Temperature (°C)
Unprotected	11	1	252.4	307	Purlin	252.4	0.4826	3.08E+07	814
				481	Girt	252.4	0.3503	2.90E+07	814
	11 and 12	2	244.8	325	Purlin	244.8	0.5967	3.40E+07	805
				340	Purlin	244.8	0.4552	3.26E+07	805
				481	Girt	244.8	0.3844	2.79E+07	805
	11, 12, and 13	3	245.6	310	Purlin	245.6	0.6614	3.31E+07	806
				337	Purlin	245.6	0.5044	3.34E+07	806
				362	Girt	245.6	0.5808	3.06E+07	806
Protected	11	4	3602	307	Purlin	3346.8	0.3345	1.95E+08	539
				481	Girt	3602	0.2309	1.64E+08	539
	11 and 12	5	3602	310	Purlin	3602	0.3896	1.99E+08	539
				481	Girt	3311.4	0.2799	1.64E+08	539
	11, 12, and 13	6	2733.5	313	Purlin	2733.5	0.3927	1.92E+08	539
				388	Girt	2733.5	0.3388	1.73E+08	539

Abaqus aborted analysis within the first four minutes for all three of the unprotected fire cases. Maximum deflections for the unprotected fire cases ranged from 330 mm (thirteen inches) to 661 mm (twenty-six inches). Abaqus also aborted analysis of Case 6, which is the protected fire case in which the three bays, Bays 11, 12, and 13, are exposed to the design fire curve, after nearly forty-six minutes. Although, maximum deflections for the Protected fire cases ranged from 228 mm (nine inches) to 406 mm (sixteen inches).

It is also observed that relatively large deformations occurred when more than two bays are exposed to a design fire such as case 3 where maximum displacement of 661 mm (twenty-six inches) occurred when three bays were on fire. This is also observed for case 6 when fire protection is utilized with maximum displacement is 392 mm (fifteen inches), therefore limiting the extent of the fire could be beneficial.

The three-dimensional modeling also helped in revealing interesting structural member interactions, which is shown in the different purlin and girder responses. This observation is lacking in the previous 2D models [25] and presents a more realistic failure response than from 2D modeling.

3.2 Limitations of Current Study

Current study did not include cases where battery fires reignite after the initial fire breakout and suppression, which has been documented to occur during several electric vehicle fires and prolonged the efforts to put out the fires [31]. While this did not occur for the Houston train fire case, the risk can be very high for large containers of wasted Li-ion batteries. How to establish a prolonged and multi-staged fire curve for battery fire is a critical information necessary for structure fire analysis.

Current study uses a hydrocarbon fire to simulate the propagation of a LIB fire, which does not include the explosive nature of a large pack lithium ion battery fire, similar to the Houston fire of the train carrying large amount of waste batteries. Currently, there is no large-scale LIB fire studies and hence, is a very critical limitation. The research team is working towards establishing experimental battery fire time histories that will be applied to the 3D structural models.

There is a quadruple increase in LIB applications, especially in large-scale utilities such as energy storages. Correspondingly, there is an increase in LIB fires, which further demonstrated the importance of such studies as demonstrated in this paper. As trains are a very likely means of transport for waste batteries, there is an urgent need to investigate LIB fires to neighboring structures. The analysis process demonstrated in current paper represent a critical first step towards the understanding of large-scale LIB fires and can be a useful approach for future fire risk evaluation of any structure types.

4. Conclusions

LIB fire due to depleted battery stockpiles has drawn critical attentions during the 2017 Houston train fire incidence. Even though fire regulations are not addressing the fire safety issues of waste LIB transportation yet, there is a need to establish a holistic approach to evaluate fire risk potentials. This paper investigated the fire risks of a steel frame structure using 3D FE modeling. The 3D analysis allowed us to visualize the selected fire scenario and helped identify the most critical members subject to battery fire and their performances. The fire study was based on the North Carolina Capital Railyard Warehouse with multiple potential train access sites.

When considering the fire safety and control of a fire, the most significant fire scenario was determined to be a battery train fire within the warehouse which could potentially be caused by thermal runaway and is more difficult to control than a conventional fire.

Based on the assumptions made and data available from the 3D finite element model, it appears that structural components would experience relatively large stresses and deflections during a design fire and the structure could potentially become unstable. The analysis appears to demonstrate that utilizing fire protection could slow the rate at which structural steel members would deflect, reduce the total deflection experienced by a structural member, and delay or prevent structural instability. The research also indicates that structural instability could occur if more than two bays are exposed to a design fire even if fire protection is utilized, therefore limiting the extent of the fire could be beneficial.

Finally, the 3D modeling reveals interesting and more realistic member interactions during the fire propagation than two-dimensional modeling.

Acknowledgements

The authors would like to extend their thanks and acknowledge the North Carolina Department of Transportation (NCDOT) for the data they provided and their collaboration. Any opinions, findings, and conclusions expressed in this paper are those of the authors and do not necessarily reflect the views of the NCDOT. The research team would like to acknowledge technical contributions from Jasmine Mira and 2020 spring senior design team members: Peter Theilgard, Marwa Elkazzaz, Seth Cathey and David Vences.

Conflict of Interest

There is no conflict of interest.

References

[1] Armand, M., Axmann, P., Bresser, D., et al., 2020. Lithium-ion Batteries- Current State of the Art and Anticipated Developments, Journal of Power Sources. 479, 228708.

[2] Notter, D.A., Gauch, M., Widmer, R., et al., 2010. Contribution of Li-ion batteries to the Environmental Impact of Electric Vehicles. Environmental Science Technologies. 44, 6550-6556.

[3] Church, C., Wuennenberg, L., 2019. Sustainability and Second Life: The Case for Cobalt and Lithium Recycling, Technical Report, International Institute for Sustainable Development (IISD). pp. 68.

[4] Federal Register, 2007. Hazardous Materials; Transportation of Lithium Batteries. 49 CFR Parts 171, 172, 173 and 175, Pipeline and Hazardous Materials Safety Administration (PHMSA), USDOT.

[5] Houston Fire Department, 2017. "Chapman Street Fire," Report No. 17-1120608, Houston Fire Department.

[6] Romo, S.N., 2020. Personal Communication, KTRK-TV.

[7] Summer, S., Maloney, T., 2017. Fire Hazard Analysis for Various Lithium Batteries, Report No. DOT/FAA/TC-16/17, US Department of Transportation.

[8] Wang, Q., Ping, P., Zhao, X., et al., 2012. Thermal Runaway Caused Fire and Explosion of Lithium Ion Battery. Journal of Power Sources. 208, 210-224.

[9] Long, Jr.R.T., Sutula, J.A., Kahn, M.J., 2014. Flammability of Cartoned Lithium Ion Batteries, the Fire Protection Research Foundation, Springer, New York.

[10] Larsson, F., Anderson, J., Andersson, P., et al., 2016. Thermal Modelling of Cell-to-Cell Fire Propagation and Cascading Thermal Runaway Failure Effects for Lithium-Ion Battery Cells and Modules Using Fire Walls. Journal of Electrochemical Society. 163(14), A2854-A2865.

[11] Blum, A.F., Long, Jr.R.T., 2016. Fire Hazard Assessment of Lithium Ion Battery Energy Storage Systems, Springer, New York.

[12] DNV-GL, 2020. McMicken Battery Energy Storage System Event Technical Analysis and Recommendations. Arizona Public Services Report No. 10209302-HOU-R-01.

[13] APTA, 2009. Recommended practice for Transit Bus Fire/Thermal Incident Investigation, APTA BTS-BS-RP-004-08.

[14] APTA, 2009. Recommended practice for Transit Bus Electrical System Requirements Related to Fire Safe-

ty, APTA BTS-BS-RP-002-07.
[15] APTA, 2009. Recommended Practice for Installation of Transit Vehicle Fire Protection Systems, APTA BTS-BS-RP-003-08.
[16] APTA, 2009. Recommended practice for Fire Safety Analysis of Existing Passenger Rail Equipment, APTA BTS-BS-RP-005-00.
[17] APTA, 2009. Recommended practice for Fire Detection System Inspection and Testing, APTA RT-SC-S-042-03.
[18] NFPA, Standard for Fixed Guideway Transit and Passenger Rail Systems, NFPA-130, National Fire Protection Association, Washington, D.C, 2020.
[19] IBC (International Building Code), 2018. International Code Council, Washington, D.C.
[20] LaMalva, K., 2018. Structural Fire Engineering, ASC/SEI Manual of Practice.
[21] MBMA, 2010. Fire Resistance Design Guide for Metal Buildings Systems, Manual, Metal Building Manufacturers Association, Ohio.
[22] MBMA, 2018. Metal Building Systems Manual, Handbook. Metal Building Manufacturers Association, Ohio.
[23] MBMA, 2018. Seismic Design Guide for Metal Building Systems, Metal Building Manufacturers Association, Third Edition, Ohio.
[24] AISC (American Institute of Steel Construction), 2017. Steel Construction Manual, 15th Edition. Chicago.
[25] Mira, J., Braxtan, N.L., Chen, S.E., et al., 2021. Battery Train Fire Risk on a Steel Warehouse Structure. Journal of Architectural Environment and Structural Engineering Research. 4, 3.
[26] Abaqus, 2018. User's Manual, Abaqus Inc., Johnston, RI.
[27] Haehler, R., 2011. Steel Design Guide 25: Frame Design Using Web-Tapered Members. Steel Design Guide Series Number 25, AISC.
[28] ASCE/SEI, 2016. American Society of Civil Engineers, ASCE Standard 7-16 Minimum Design Loads and Associated Criteria for Buildings and Other Structures. Virginia.
[29] EN 1993-1-1, 2005. Eurocode 3: Design of Steel Structures - Part 1-2: General rules – Structural Fire Design. Brussels: Comité Européen de Normalisation.
[30] EN 1991-1-2, 2009. Eurocode 1: Actions on Structures - Part 1-2: General Actions - Actions on Structures Exposed to Fire. Brussels: Comité Européen de Normalisation.
[31] Sun, P., Huang, X., Bisschop, R., et al., 2020. A Review of Battery Fires in Electric Vehicles. Fire Technology. 56, 1361-1410.